Riparian ecosystems mapping at fine scale: a density approach based on multi-temporal UAV photogrammetric point clouds

Remote Sensing in Ecology and Conservation
Open Access
ZSL LET'S WORK FOR WILDLIFE

ORIGINAL RESEARCH

Riparian ecosystems mapping at fine scale: a density approach based on multi-temporal UAV photogrammetric point clouds

Elena Belcore & Melissa Latella

DIATI, Department of Environment, Land and Infrastructure Engineering, Politecnico di Torino, Corso Duca degli Abruzzi, 24, 10129, Torino, Italy

Keywords
individual tree, ITD, multi-temporal, photogrammetry, points density approach, Riparian ecosystems, treetop, UAV

Correspondence
Elena Belcore, DIATI, Department of Environment, Land and Infrastructure Engineering, Politecnico di Torino, Corso Duca degli Abruzzi, 24, 10129 Torino, Italy.
Tel: +39 0110907687; E-mail: elena.belcore@polito.it

Editor: Mat Disney
Associate Editor: Karen Anderson

Received: 23 September 2021; Revised: 16 February 2022; Accepted: 22 March 2022

doi: 10.1002/rse2.267

Abstract

In recent years, numerous directives worldwide have addressed the conservation and restoration of riparian corridors, activities that rely on continuous vegetation mapping to understand its volumetric features and health status. Mapping riparian corridors requires not only fine-scale resolution but also the coverage of relatively large areas. The use of Unmanned Aerial Vehicles (UAV) allows for meeting both conditions, although the cost-effectiveness of their use is highly influenced by the type of sensor mounted on them. Few works have so far investigated the use of photogrammetric sensors for individual tree crown detection, despite being cheaper than the most common Light Detection and Ranging (LiDAR) ones. This work aims to improve the individual crown detection from UAV-photogrammetric datasets in a twofold way. Firstly, the effectiveness of a new approach that has already achieved interesting results in LiDAR applications was tested for photogrammetric point clouds. The test was carried out by comparing the accuracy achieved by the new approach, which is based on the point density features of the analysed dataset, with those related to the more common local maxima and textural methods. The results indicated the potentiality of the density-based method, which achieved accuracy values (0.76 *F*-score) consistent with the traditional methods (0.49–0.80 *F*-score range) but was less affected by under- and over-fitting. Secondly, the potential improvement of working on intra-annual multi-temporal datasets was assessed by applying the density-based approach to seven different scenarios, three of which were constituted by single-epoch datasets and the remaining given by the joining of the others. The *F*-score increased from 0.67 to 0.76 when passing from single- to multi-epoch datasets, aligning with the accuracy achieved by the new method when applied to LiDAR data. The results demonstrate the potential of multi-temporal acquisitions when performing individual crown detection from photogrammetric data.

Introduction

Riparian corridors are ecotones at the interface between rivers and the surrounding lands, within which a smooth transition between aquatic and terrestrial habitats occurs (Malanson, 1993; Naiman et al., 2005). In these areas, the water table shows both seasonal trends and significant stochastic fluctuations driven by precipitation, leading to a variable and heterogeneous distribution of nutrients and soil moisture, which promotes biodiversity and the establishment of numerous ecological communities (Malanson, 1993). Floods influence the riparian communities by transporting nutrients and seeds inland but also disrupting habitats, causing anoxia and uprooting plants (Camporeale et al., 2013). In such chaotic dynamics, vegetation gives crucial feedback by affecting the water flow and sediment transport and contributing to a large part of the ecosystem services provided by the riparian ecotones. For instance, the alternation between vegetation growth and flood-induced uprooting promotes CO_2

sequestration from the atmosphere (Salerno et al., 2020), whereas vegetation growth on steep riverbanks increases their consolidation, preventing erosion (Capon & Pettit, 2018; Solari et al., 2016).

Several directives worldwide have been drawn up in recent years to protect the ecological richness of riparian corridors and maintain their functionalities. In Europe, the conservation and management of riparian areas and rivers have been addressed progressively since the 1990s through policies and legal acts: the Habitat directive (Council Directive 92/43/EEC) counts riparian areas among the habitats to be protected, mapped and monitored; the Water Framework directive (2000/60/EC) legally bounded the Member States to assess the ecological status of river and riverine habitats; the Council Regulation (EC) 73/2009 enforced the definition of buffer zones to protect watercourse from agricultural runoff by 2012 (JRC, 2011).

In addition to protection, rivers and riparian habitats often need restoration (Capon & Pettit, 2018). Many countries and institutions are following this trajectory by setting up national or international programs to monitor riparian ecosystems' status and share the best practices for riparian restoration (e.g. the EU Biodiversity Strategy for 2030).

However, conservation, restoration, management and the modelling underlying these activities demand the assessment of riparian vegetation parameters, therefore urgently requiring the mapping of biophysical properties both at the scale of a single tree and at larger spatial extents (Souza & Johansen, 2009). Recently, new tools for habitat mapping have taken hold. Unmanned Aerial Vehicles (UAV), also known as Remotely Piloted Aircraft Systems (RPAS), have gained the approval of the scientific community, becoming a common approach for information gathering and data collection in a wide range of environmental studies (Belcore et al., 2021; D'Oleire-Oltmanns et al., 2012; Ferreira et al., 2020; Shi et al., 2020; Sothe et al., 2019; Takahashi Miyoshi et al., 2020; Xu et al., 2020). The UAVs meet the needs for habitat mapping at a finer scale. Indeed, the time-saving survey, compared to traditional field surveys, is one of the distinctive features of UAV systems. An additional factor contributing to their increasing favour is the wide range of mountable sensors able to collect Very High Resolution (VHR) data, such as Light Detection and Ranging (LiDAR), Synthetic Aperture Radar (SAR) and optical cameras (De Luca et al., 2019; D'Oleire-Oltmanns et al., 2012; Hruska et al., 2012; Skoglar et al., 2012). VHR sensors permit very fine-scale environmental studies, reaching single element detail, such as individual trees, shrubs and animals.

Previous studies have primarily defined the identification of single tree canopies within an ecosystem as Individual Tree Detection (ITD), Individual Crown Detection (ICD) or Individual Tree Crown Detection (ITCD). Several ITD methods for automatically detecting single crowns from UAV sensed data currently exist. (Dong et al., 2020) identified three categories for the ITC methods suitable for LiDAR data:

i. The point clouds-based methods, which take advantage of the three-dimensionality of LiDAR data and are mainly represented by voxel segmentation and clustering techniques (Dong et al., 2020);
ii. The raster-based methods, which generally use normalised digital surface model (nDSM), or so-called canopy height model (CHM) (Mohan et al., 2017; Vastaranta et al., 2012);
iii. The methods combined on point clouds and raster data, consisting of a miscellaneous approach and generally using *a priori* information. Such techniques are particularly efficient for detecting understory tree crowns.

Although these categories are meant for LiDAR datasets, the methods also apply to point clouds derived from aerial photogrammetry. Unlike LIDAR sensors, optical cameras are not multi-return and provide users with information from the top of the crowns only (Mohan et al., 2017; Pearse et al., 2018). This results in a lack of information about the vertical development of canopies and the understory vegetation by photogrammetric clouds. In addition, photogrammetric clouds are generally noisier than LiDAR ones. This aspect is exacerbated in high-density forested areas since the photogrammetric techniques fail to find homologous points in the frames due to the poor variability of the scene and the dynamism of wind-shaken leaves. These characteristics generally make ITD point cloud-based techniques less suitable for aerial photogrammetric point clouds.

Raster-based methods are popular ITD solutions for optical data (Mohan et al., 2017; Vastaranta et al., 2012). Indeed, raster-based methods were born for optical imagery and today are the most mature and frequent approach for ITD from photogrammetric datasets. These methods require the translation of the photogrammetric point cloud into 2D information through a rasterisation process. The result is then normalised in a CHM (Lindberg & Holmgren, 2017), which is the starting data for many raster-based approaches.

One of the most well-known methods for delineating crowns consists of detecting the tree apices from a point cloud or CHM and then, expanding outward from those peaks (i.e. input seeds). Consequentially, the precision of the ITD is strongly affected by the quality of the treetop detection. A common method for the treetop definition is

through local maxima analysis, based on LiDAR point clouds or 2D-CHM, using a fixed constant size window or a variable one (Roussel et al., 2020). Once identified the treetops, the crowns are delineated starting from it by working on contiguous pixels (De Luca et al., 2019; Dong et al., 2020; Torres-Sánchez et al., 2015; Wang et al., 2019) and grouping them according to a variety of criteria, such as adjacent point distance from the treetop (Li et al., 2012) and region growing (Dalponte & Coomes, 2016). (Eysn et al., 2015) benchmarked eight airborne laser scanning (ALS)-based single tree detection methods, five of them are based on local maxima. This method for treetop detection is implemented in several softwares and packages, for example, the R package lidR (Roussel et al., 2020) and Pycrown (Zörner et al., 2018). Generally, the local maxima algorithm generates advantageous results in uniform forest stands, with definite peaks, such as coniferous ones. It performs worse when employed to multi-layered stands or interlocking crowns (Ayrey et al., 2017), such as those of broadleaf-dominated river banks. Some authors have proposed textural-based approaches that avoid the use of seeds, but the commission error of such methods is usually high (Belcore et al., 2020; Dong et al., 2020). Other recent methods for tree crown segmentation that do not use treetop as seeds rely on nearest neighbour analysis (Vega et al., 2014), single-processor tree segmentation algorithm (Hamraz et al., 2017) and clustering point clouds slices (Ayrey et al., 2017).

Besides the ITD solutions avoiding the detection of tree apices, a parallel research path aims to improve ITD by investigating treetop detection methods alternative to the local maxima ones. Some authors attempted to consider the brightest pixels in a given neighbourhood as seeds and then generate the crowns based on the brightness level of the surrounding pixels (Bottai et al., 2013; Panagiotidis et al., 2017; Pouliot et al., 2002; Sačkov et al., 2014; Vastaranta et al., 2012; Wolf & Heipke, 2007). However, despite the effectiveness of this method, it can be applied only on raster data, and performs worse on deciduous stands.

Recently, a new straightforward treetop detection method has been developed by (Latella et al., 2021). It is based on the point-density properties of the input cloud, and it has been successfully applied over LiDAR data. A detailed explanation is provided in the Methods section.

It has previously been observed that ITD might benefit from multi-temporal datasets (Belcore et al., 2021; Michez et al., 2016; Shi et al., 2020; Takahashi Miyoshi et al., 2020). For instance, (Michez et al., 2016) found that the redundancy given by multi-temporal acquisitions can improve species discrimination and support the assessment of trees' health conditions. Similarly, (Takahashi Miyoshi et al., 2020) noted that combining datasets acquired at different time steps can reduce the influence of weather and enhance species identification. Nevertheless, as far as we know, no studies have investigated the advantages of multi-temporality for ITD so far. For the present work, we assumed photogrammetric point clouds can simulate the points distribution of LiDAR cloud, which captures richer sub-canopy structural information, through varying the canopy penetration. This can be achieved with data collected in different intra-annual phenological conditions. According to this assumption, since the density-based ITD method is designed for LiDAR, we expect multi-temporal photogrammetric cloud having information about the lower layers and improving the performance of the density-based approach.

Considering the need for monitoring, protecting and mapping riparian ecosystems, this work aims to improve the individual crown detection from UAV-photogrammetric datasets by testing the effectiveness and precision of the density-based approach, which was developed for ITD over LiDAR point clouds by (Latella et al., 2021). Furthermore, it aims to evaluate the contribution of intra-annual multi-temporality in the ITD process to provide indications to better plan UAV-photogrammetric surveys. The evaluation was realised in terms of accuracy (i.e. correctly detected treetop) and precision (i.e. treetop position).

Materials and Methods

Study site

The study site is an alpine riparian area of approximately 0.7 ha near the town of Salbertrand in the Susa Valley (45.074000 N, 6.892200 E, Western Alps, Italy), at the elevation of 1000 m a.s.l. (Fig. 1). It is part of the area described in Belcore et al. (2021), characterised by a warm and temperate climate, an average annual temperature of about 8.2°C, and an annual average precipitation of 701 mm (considering the period: 1993–2017).

The site is located within the floodplain of the Dora Riparia River, which rises in the Cottian Alps and ends at the confluence with the Po River, in the city of Turin, after 101 km. Vegetation entirely covers the site and encompasses tree species typical of riparian areas. It comprises shrubby willows (*Salix eleagnos, Salix purpurea*), Sea buckthorns (*Hippophae rhamnoides*) and young individuals of poplars (*Populus nigra*) close to the main channel, whereas it is gradually replaced by trees having mature age and considerable size belonging to hardwood communities such as *Salix alba*, *Fraxinus excelsio*r, *Betula pendula*, *Populus nigra* and *Pinus silvestris* moving landward. This vegetation gradient has been confirmed by

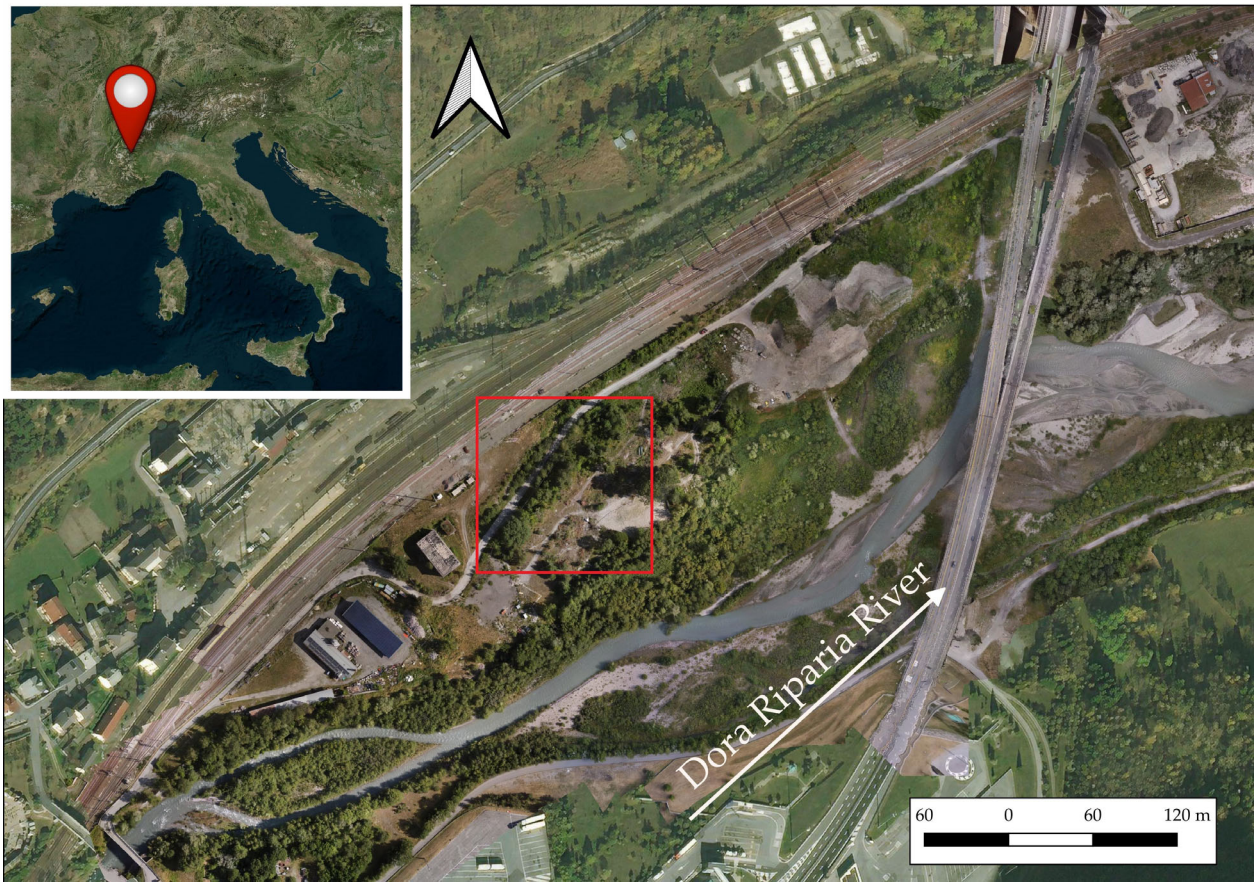

Figure 1. The study area. Visualization of the RGB orthophoto from epoch 2 completed by satellite imagery from Bing©. The red polygon indicates the survey extent.

visual inspection of high-resolution orthophotos and three field surveys performed throughout 2020.

Available data

The data underlying this work belongs to the dataset described in (Belcore et al., 2021), consisting of very high-resolution optical data collected by multirotor-unmanned aerial vehicle (UAV) technology. The dataset was created after three subsequent UAV campaigns that caught relevant time, defined as *epochs*, of the year 2020 from a phonological perspective: (i) the beginning of green-up (epoch 1, March), (ii) the flowering of Salix spp. (epoch 2, June) and (iii) the maximum crown development (epoch 3, July).

The sensors mounted on the UAV provide multispectral information of the red (R), green (G), blue (B), near-infrared (NIR) and red-edge (REDGE) bands of the electromagnetic spectrum. The collected data were processed through a standard Structure from Motion (SfM) workflow (Turner et al., 2012) to provide, among others, a three-dimensional point cloud, a digital surface model (DSM), and RGB and RGNIR orthomosaics with 8 centimetres accuracy for each of the investigated epoch. Further information about data collection and processing are reported by (Belcore et al., 2021), whilst the SfM elaboration parameters and their results are summarised in the Appendix S1.

Algorithms

With the aim of evaluating the so-called *density-based approach* when applied to photogrammetric data, we tested three different algorithms on the same dataset.

The density-based approach has been proposed by (Latella et al., 2021) and constitutes the core of our analysis. It has been developed as a Matlab script that processes LiDAR point clouds and returns the position of trees within a study site. Unlike most other ITD methods, which detect trees according to local maxima in the canopy surface model, this algorithm relies on a density-based approach, namely identifying tree stems at the local

areal-density maxima of the input point cloud. To summarise, the algorithm removes the cloud's outliers and applies a height threshold to remove understory bushes and grass. In the original version, this threshold was equal to 1.4 m, but we changed it to 0.4 m according to the study site's characteristics. Subsequently, it determines the optimal neighbourhood's size to compute the local areal densities and detects the stems. Later, the detected stems are filtered to remove the double-counted trees based on the typical stem spacing in the investigated area, which we set equal to 2.5 m according to field observations. The algorithm may eventually remove anthropic objects standing among the trees (e.g. fences), but we did not use this functionality since the study site is entirely wild.

The second tested algorithm is a local maxima method implemented in the Python environment by (Zörner et al., 2018) with the library Pycrown, in the version developed by (Dalponte & Coomes, 2016).

The third tested ITD method is textural-based, and it does not require input seeds. It was initially applied and explained in (Belcore et al., 2021). It performs a multiresolution segmentation analysis over the CHM, the spectral and textural information calculated over the NIR and visible bands. In this case, the ITD was performed using eCognition Developer software (version 10.1).

Methodology: model evaluation

To evaluate the performance of the density-based algorithm applied to photogrammetric 3D data, we first tested it for seven different scenarios described in Table 1. The first three scenarios correspond to the individual epochs, the fourth, fifth and sixth ones describe the combination of point clouds from two epochs, whereas the seventh scenario is given by merging all the 3D data into a single point cloud. We also applied the other two algorithms to obtain benchmark data.

In agreement with similar works (Ke & Quackenbush, 2011), the ITD effectiveness was assessed by evaluating the correspondence between manually defined reference tree crowns and the algorithm-detected trees. For this purpose, we selected 64 tree crowns randomly spread all over the study site (Fig. 2). Since crowns definition in the field would be very difficult due to the thick undergrowth vegetation, 100 points were randomly selected in the study area by applying the Gdal *Random points in extent* algorithm in Qgis software (version 3.4.3.8). Then each point was visually analysed and, in the case, it laid over a crown, it was manually digitalized on the basis of the R-G-B and R-G-NIR orthomosaics.

Table 1. Analysed scenarios.

Scenario ID	Epoch
Scenario 1	Epoch 1
Scenario 2	Epoch 2
Scenario 3	Epoch 3
Scenario 4	Epochs 1, 2
Scenario 5	Epochs 1, 3
Scenario 6	Epochs 2, 3
Scenario 7	Epochs 1, 2, 3

Unlike the textural-based approach, which computes polygons representing the crowns, the outputs of density-based and local maxima algorithms are points representing the treetops. Therefore, the centroids of the polygons identified by the textural-based algorithm were taken as the treetops for the comparison to the other algorithms. For each delineated crown, we assigned one of the following ratings: (i) true positive (TP), if the algorithm correctly detects it; (ii) false negative (FN), if the algorithm omits the tree; and (iii) false positive (FP), if the algorithm attributes more than one tree to the reference crown. Based on these ratings, we computed the standard metrics for accuracy assessment (Li et al., 2012), namely the *recall* (r), representing the rate of tree detection, the *precision* (p), indicating the correctness of detection, and the F-score, which refers to the overall detection accuracy:

$$r = \frac{\mathrm{TP}}{\mathrm{TP}+\mathrm{FN}}; p = \frac{\mathrm{TP}}{\mathrm{TP}+\mathrm{FP}}; F_{\mathrm{score}} = 2\frac{r \cdot p}{r+p} \quad (1)$$

Optimal values of precision and recall are expected to be at least around 0.70. Finally, we estimated the residuals between the centroids of the reference crowns (R_i) and the algorithm-detected treetops (C_i) for the n True Positive of Scenario 7 through the Root Mean Square Error (RMSE)

$$\mathrm{RMSE}(m) = \sqrt{\frac{\sum_{i=1}^{n}(R_i - C_i)^2}{n}}, \quad (2)$$

Results

Table 2 presents the analysis results of the single epoch scenarios (1, 2 and 3) and the multi-epoch scenarios (4, 5, 6 and 7).

Comparing the three analysed ITD methods of Scenario 7 emerged similar performances of local-maxima algorithms, which reached 0.80 F-score, and the density-based algorithm with 0.76 F-score. The textural-based algorithm returned the worst results with an F-score of 0.49 and an extremely low precision value. With its 0.70 recall, the local maxima method shows a tendency to under-segmenting (i.e. omitting some crowns). Differently, the density-based approach appears more balanced (Fig. 3),

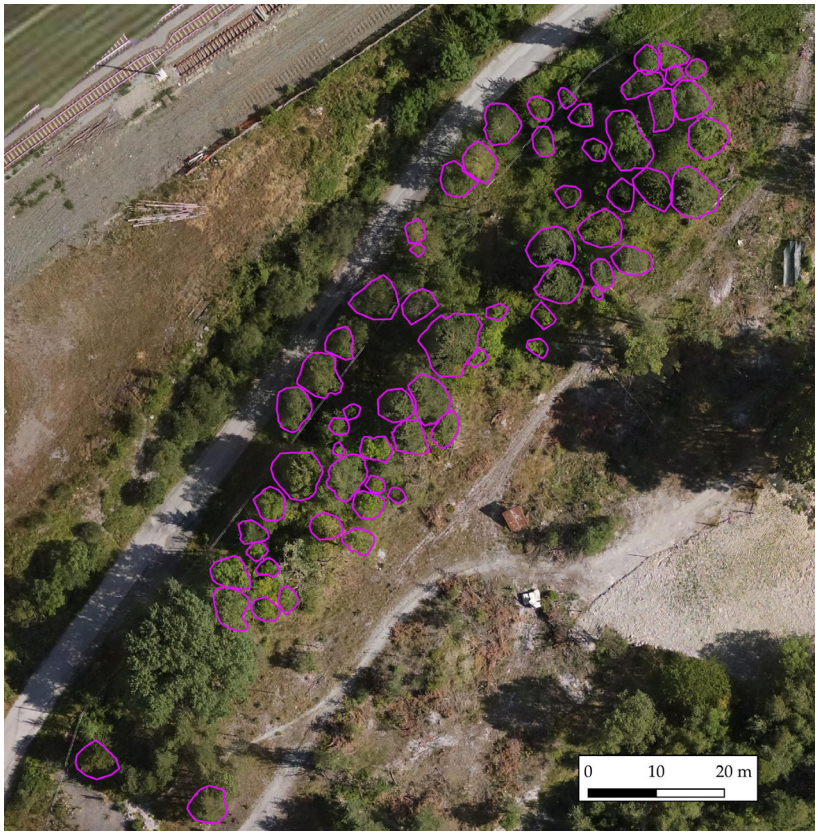

Figure 2. The reference crowns.

Table 2. Results of single-epoch (1, 2 and 3) and multi-epochs (4, 5, 6 and 7) scenarios.

Algorithm	Scenario	TP	FN	FP	r	p	F_{score}	RMSE (m)
Density based	1	32	26	6	0.55	0.84	0.67	1.04
	2	27	26	11	0.51	0.71	0.59	1.04
	3	46	42	3	0.52	0.94	0.67	1.15
	4	41	22	1	0.65	0.98	0.78	1.24
	5	35	8	21	0.81	0.63	0.71	0.82
	6	37	22	5	0.63	0.88	0.73	1.21
	7	39	11	14	0.78	0.74	0.76	1.25
Textural based	1	30	20	14	0.62	0.54	0.58	0.92
	2	14	33	17	0.30	0.45	0.36	0.78
	3	17	21	26	0.27	0.45	0.40	0.62
	4	26	16	22	0.62	0.54	0.58	0.78
	5	17	27	20	0.39	0.46	0.42	0.79
	6	26	19	19	0.58	0.58	0.58	0.87
	7	19	5	40	0.79	0.32	0.49	0.78
Local maxima	1	18	45	1	0.29	0.95	0.44	1.52
	2	20	38	6	0.34	0.77	0.48	0.89
	3	22	41	1	0.34	0.35	0.96	1.26
	4	21	42	1	0.33	0.95	0.49	1.43
	5	24	39	1	0.38	0.96	0.55	1.29
	6	24	40	0	0.38	1.00	0.55	1.47
	7	43	19	2	0.69	0.96	0.80	1.16

showing close precision and recall values, respectively, 0.74 and 0.78. A similar tendency is recorded in scenario 3, whilst the density-based method outperformed the local maxima and the textural approaches in the remaining scenarios (i.e. 1, 2, 4, 5 and 6), reaching 0.78 of *F*-score in scenario 4. We note that the local maxima algorithm unexpectedly reached 0.96 of *F*-score in Scenario 3 and that this performance is not in line with the other single epoch scenarios. The scenario 7 RMSE of the density-based and local maxima algorithms exceeded 1 m (1.25 and 1.16 m, respectively) over an average of 14.68 m of reference crown circumference (Fig. 4). The textural-based algorithm returned only 0.78 m of RMSE, being the best centroids residuals results, although associated with a very poor *F*-score (0.46). This trend is confirmed in the other multi-epochs and single-epoch scenarios. Although less accurate, the true positives are precisely identified using the textural algorithm.

Considering the performances of the density-based approach throughout the scenarios, the similarity among the results of single epoch scenarios is evident: the *F*-score is 0.67 for scenarios 1 and 3, and slightly lower for scenario 2 (0.59). The accuracy considerably increased in the multi-temporal scenarios, reaching *F*-score equal to

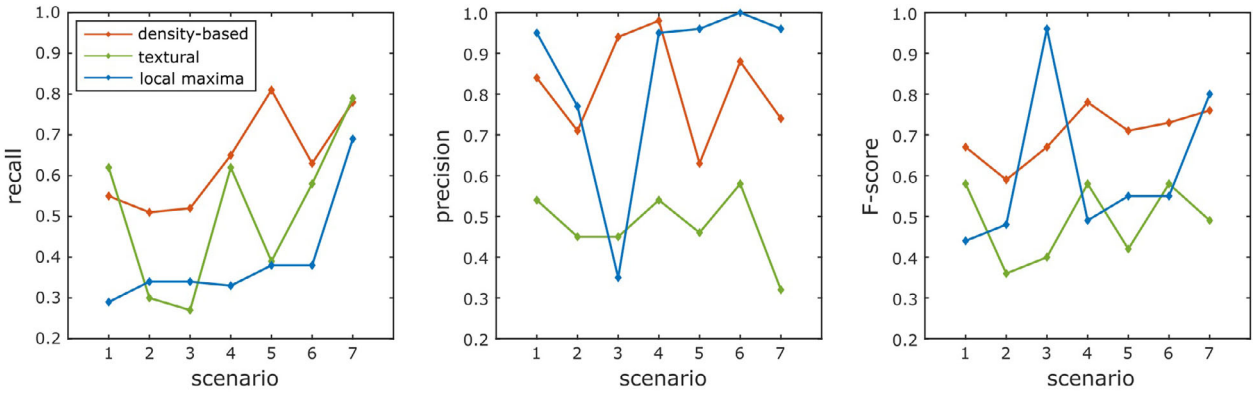

Figure 3. Graphical restitution of the accuracy measures of the analysed ITD methods.

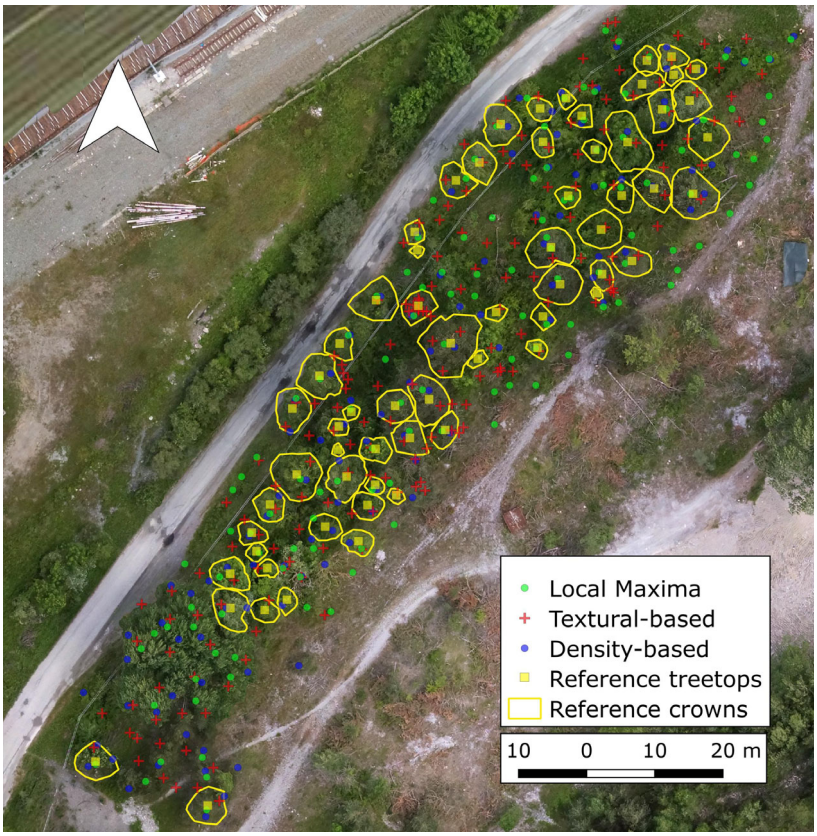

Figure 4. Result of treetops detection. The reference crowns (yellow) and treetop (yellow squares), are compared with the local maxima (green dots), textural-based (red dots) and the density-based (blue dots) approaches.

0.78 and 0.76 in scenarios 4 and 7, respectively. The density-based approach in single epoch scenarios clearly tends to under-segmenting, as the achieved precision and recall indicate. Indeed, the false-negative trees overcome the true-positive ones, and consequentially the recall is consistently lower than the precision. As mentioned before, the density-based method in the multi-temporal scenario 7 is better balanced, showing no particular predisposition to over- or under-segmentation.

A comparison between the performances of the density-based approach in two-epochs scenarios (i.e. 4, 5 and 6) and the three-epochs scenario 7, reveals little difference. The *F*-score moved from 0.78 (scenario 4) and 0.76 (scenario 7), suggesting no or slight improvement by

adding the third epoch. The method maintains the balance between the precision and recall values also for two-epochs scenarios.

Overall, these results indicate that the analysed ITD approaches take advantage of multi-temporality and that two epochs are sufficient for accurate results.

Discussion

The study mainly aimed to assess the applicability of a novel density-based approach for treetop detection and their localization, which has been applied only on aerial LiDAR data so far. The present work tests it on a UAV-photogrammetric point cloud dataset for the first time, exploring the window of opportunity of using photogrammetry for ITD in riparian environments.

We compared the novel approach with consolidated methods for treetop detection, such as local maxima algorithm and textural-based analysis. The obtained results outperform the textural-based results, whilst being in line with those of the local maxima algorithm, although the density-based accuracy is slightly lower than this latter because of a higher number of false positives. Such difference might be traced back to the nature of the novel algorithm. Indeed, the density-based approach was developed for LiDAR data applications and specifically intended to detect understory and dominating layer crowns. However, the photogrammetric points clouds do not provide the user with such information leading the algorithm to detect false positives in high-density point clouds. This tendency is further exacerbated by the noise that typically affects photogrammetric point clouds and that is even more noticeable over the vegetation and magnified by the multi-temporality. Table 2 and Figure 3 show that textural method results are always poorer than the others. The local maxima method works well or better than density-based when the vegetation is at its maximum seasonal development (scenarios 3 and 7). The density-based has a good performance for single epochs and its *F*-score is always above 0.7 in multitemporal cases. It shows a constancy in generating results with a good *F*-score, while the performances of the local maxima and textural-based algorithms appear highly conditioned by the phenological stage of the vegetation.

The comparison between the density-based results from the photogrammetric dataset and the LiDAR one from (Latella et al., 2021) shows consistency of the achieved precision values (ranging from 0.71 to 0.94 and from 0.75 to 1.00 for photogrammetric and LiDAR data, respectively). This indicates no or slight tendency to over-detection, suggesting that the density-based approach might be used in synergy with the seed-based methods to pre-process the point clouds and yield the seeds starting from which delineating the tree crowns.

In the work by (Latella et al., 2021), the recall values are higher than 0.78 for 11 of the 12 study areas, while they are within the range of 0.51–0.55 when applied to single-epoch photogrammetric scenarios 1 to 3, and equal to 0.78 if considering Scenario 7. As aforementioned, the first three scenarios are characterised by point clouds representing the upper layer of vegetation not providing information that is fundamental for the proper working of the density-based approach, which usually investigates the vegetation from the upper canopy to the ground level. By merging the clouds from the previous scenarios, Scenarios 4, 5, 6 and 7 present information about the lower layers improving the performance of the density-based approach and aligning the recall value to those obtained from its applications over LiDAR data. In light of these considerations, the photogrammetric-related worse performance in terms of *F*-score is completely explained and mainly attributable to the lower recall and the higher noise of the photogrammetric cloud.

The LiDAR dataset analysed by (Latella et al., 2021) and the photogrammetric dataset of scenario 1 were collected during the vegetative rest (respectively February and March) when the crowns have no leaves. Since the leaves are the primary source of noise in 3D models (both photogrammetric and LiDAR sensed), treetop detection algorithms may be expected to better perform on leaf-off conditions. However, photogrammetry yields less information about vegetation structure than LiDAR data, and the leaf-off condition, which is associated with a lower number of points representing a given tree, may further worsen the tree identification. As a balance of these two opposing processes, no significant differences were found in the accuracies of scenario 1 and scenario 3 (maximum crown development). Moreover, although both scenario 1 of the present work and (Latella et al., 2021) refer to leaf-off conditions, a sharp difference can be found between the *F*-scores (0.67 and 0.76, respectively), likely related to the noise of the photogrammetric point cloud. This comparison further highlights the superiority of the ITC based on LiDAR data rather than the ITC relying on one-time photogrammetric acquisitions.

The current study set out with the additional aim of assessing the role of multi-temporality in treetop identification. The density-based algorithm was applied on three single-epoch scenarios (1, 2 and 3) and on a multi-epoch scenario that merged the single-epoch photogrammetric point clouds. The findings revealed that the *F*-score increases from 0.67 to 0.76 with the information collected from different times of the year, aligning with the accuracy met by the LiDAR-based ITC. The improvement is mainly due to point redundancy and the creation of

in-depth information for the merged dataset. Thus, the critical role of multi-temporality in ecosystem monitoring and pattern classification is consolidated. Nevertheless, few scientific studies about multi-temporality in treetops and ITD analysis have been carried out so far. The results obtained by the current work prove that multi-temporality can positively influence segmentation too. This is an interesting issue for future research in remote sensing for riparian and forest ecosystems monitoring.

The *F*-score values of two-epochs scenarios, compared to the one of three-epochs scenario, suggest that two surveys throughout the phenophase might be sufficient, whereas a third epoch might add noise to the merged point cloud, resulting in worse ITD. Further investigations should focus on identifying the best phenological phases for data collection. Currently, from the available data, we may assume that the leaf-off stage is fundamental, but we are still not certain whether it should be paired to the biomass peak phase (epoch 3) or late reawakening stage (epoch 2). Indeed, the *F*-scores of scenarios 4 (epochs 1 and 2) and 5 (epochs 1 and 3), respectively, 0.78 and 0.71, seem to indicate that the biomass peak phase, when crowns interlock is more evident, introduces too much noise in the cloud, but this hypothesis certainly needs further investigation.

Since the density-based algorithm here used was firstly created to work on information about the canopy and under-canopy vegetation structures, (Latella et al., 2021) assumed that it might not be suitable to analyse photogrammetric point clouds. The present work partially disproves this assumption demonstrating that it can reach accuracy values that are lower, yet acceptable, than the traditional methods when applied to single epoch photogrammetric point clouds, but comparable performances when multitemporal data are used. In the former case, the algorithm resembles the functioning of the local maxima approach as the highest areal point density is associated with the highest curvature of the canopy surface, in turn, located at the individual crown peaks. Indeed, the points distribution and density are not homogeneous in SfM-point clouds, since they are influenced by the automatic conjugate features detection, for example detected by the Scale-invariant feature transform algorithm, SIFT (Lowe, 1999), and the dense matching procedures, performed with Multi-View Stereo algorithms, MVS (Seitz et al., 2006). The detection of features generally better succeeds in regions with good contrast and varying texture (Lingua et al., 2009; Nyimbili et al., 2016). A strong relationship between the pixel size and the texture has been reported in the literature: the higher the spatial resolution, the higher the textural variability (Nyimbili et al., 2016). In the scenes where there are homogeneous dark areas (such as shadows) and moving objects (like streams or wind-shake leaves), the features detection algorithms are less performant, and, consequentially, fewer points are present in the final point cloud. Therefore, the very high spatial resolution of the dataset, the texture of the canopies, and the shaded pixels between the single tree crowns could be the primary factors causing a higher point density in correspondence of treetops and, in turn, the good performances of density-based ITC algorithm on photogrammetric point clouds.

Moreover, the present work also found that merging the datasets from different periods provides some under-canopy information, significantly improving the accuracy of the density-based approach. Indeed, the winter-collected dataset (i.e. scenario 1) likely provided points of lower branches and the ground, available due to the absence of leaves.

To sum up, the discussed results are significant in at least two major respects: (i) the effectiveness of a novel approach for ITC on a photogrammetric dataset, and (ii) the positive impact of the multi-temporal approach in treetops detection and ITC. Moreover, the very same results lead to the inescapable efficiency comparison of UAV-mounted optical and LiDAR sensors. LiDAR data is considered more accurate than the SfM-based approaches because LiDAR can penetrate tree crowns and obtain information about trunks and lower forest strata (Moe et al., 2020), but LiDAR technologies are generally more expensive than optical ones (Pearse et al., 2018; Vastaranta et al., 2012) and require UAV with high payload capacity. In the present work, density-based photogrammetric performances proved to be at the LiDAR performances level by gathering much information collected at different times of the year was necessary. In light of these considerations, we believe that two data collection campaigns are sufficient for accurate treetop detection with density-based approach, which should be realised within the same year. Clearly, the riparian vegetation dynamics may alter the conditions between the two data collection compromising multi-temporal studies. However, unless disastrous events occur, the differences between the surveys are negligible compared to the timescale of forests dynamics. The choice between multiple optical data collection campaigns and a single LiDAR data acquisition requires a cost–benefit analysis.

Conclusions

The European Habitat Directive requires the Member States to implement surveillance of the conservation status of habitats of Community Interest and provides monitoring guidelines regarding the data collection at site level. In this framework, the UAV systems for remote sensing play a crucial role in speeding up and facilitating

field surveys. The data analysis realm should keep pace with instrument innovation. The density-based algorithm was developed with the particular purpose of studying riparian vegetation at the single tree crown level from 3D data. Although the current study is one of the preliminary tests run, the results are promising. The authors intend to implement and improve the algorithm and test it on more extensive and heterogeneous areas.

Acknowledgements

Computational resources were provided by HPC@POLITO, a project of Academic Computing within the Department of Control and Computer Engineering at the Politecnico di Torino (http://www.hpc.polito.it). Data were collected within the frame of the technical and scientific partnership between Politecnico di Torino and TELT (Tunnel Euralpin Lyon-Turin).

Author's Contribution

EB and ML conceived the ideas; designed methodology; collected and analysed the data; and wrote the manuscript. All authors contributed critically to the drafts and gave final approval for publication.

Data Availability Statement

The algorithm by Latella et al., 2021 is openly available in Zenodo repository at https://doi.org/10.5281/zenodo.4421030, while the dataset is openly available at 10.5281/zenodo.5930401.

References

Ayrey, E., Fraver, S., Kershaw, J.A., Kenefic, L.S., Hayes, D., Weiskittel, A.R. et al. (2017) Layer stacking: a novel algorithm for individual Forest tree segmentation from LiDAR point clouds. *Canadian Journal of Remote Sensing*, **43**, 16–27. https://doi.org/10.1080/07038992.2017.1252907

Belcore, E., Pittarello, M., Lingua, A.M. & Lonati, M. (2021) Mapping riparian habitats of Natura 2000 network (91E0*, 3240) at individual tree level using UAV multi-temporal and multi-spectral data. *Remote Sensing*, **13**, 1756. https://doi.org/10.3390/rs13091756

Belcore, E., Wawrzaszek, A., Wozniak, E., Grasso, N. & Piras, M. (2020) Individual tree detection from UAV imagery using Hölder exponent. *Remote Sensing*, **12**, 2407. https://doi.org/10.3390/rs12152407

Bottai, L., Arcidiaco, L., Chiesi, M. & Maselli, F. (2013) Application of a single-tree identification algorithm to LiDAR data for the simulation of stem volume current annual increment. *JARS*, **7**, 073699. https://doi.org/10.1117/1.JRS.7.073699

Camporeale, C., Perucca, E., Ridolfi, L. & Gurnell, A.M. (2013) Modeling the interactions between river morphodynamics and riparian vegetation: river morphodynamics and riparian zone. *Reviews of Geophysics*, **51**, 379–414. https://doi.org/10.1002/rog.20014

Capon, S.J. & Pettit, N.E. (2018) Turquoise is the new green: restoring and enhancing riparian function in the Anthropocene. *Ecological Management and Restoration*, **19**, 44–53. https://doi.org/10.1111/emr.12326

Dalponte, M. & Coomes, D.A. (2016) Tree-centric mapping of forest carbon density from airborne laser scanning and hyperspectral data. *Methods in Ecology and Evolution*, **7**, 1236–1245. https://doi.org/10.1111/2041-210X.12575

De Luca, G., João, M.N., Cerasoli, S., Araújo, J., Campos, J., Di Fazio, S. et al. (2019) Object-based land cover classification of Cork oak woodlands using UAV imagery and Orfeo ToolBox. *Remote Sensing*, **11**, 1238. https://doi.org/10.3390/rs11101238

D'Oleire-Oltmanns, S., Marzolff, I., Peter, K.D. & Ries, J.B. (2012) Unmanned aerial vehicle (UAV) for monitoring soil erosion in Morocco. *Remote Sensing*, **4**, 3390–3416. https://doi.org/10.3390/rs4113390

Dong, T., Zhang, X., Ding, Z. & Fan, J. (2020) Multi-layered tree crown extraction from LiDAR data using graph-based segmentation. *Computers and Electronics in Agriculture*, **170**, 105213. https://doi.org/10.1016/j.compag.2020.105213

Eysn, L., Hollaus, M., Lindberg, E., Berger, F., Monnet, J.-M., Dalponte, M. et al. (2015) A benchmark of Lidar-based single tree detection methods using heterogeneous Forest data from the alpine space. *Forests*, **6**, 1721–1747. https://doi.org/10.3390/f6051721

Ferreira, M.P., de Almeida, D.R.A., de Papa, D.A., Minervino, J.B.S., Veras, H.F.P., Formighieri, A. et al. (2020) Individual tree detection and species classification of Amazonian palms using UAV images and deep learning. *Forest Ecology and Management*, **475**, 118397. https://doi.org/10.1016/j.foreco.2020.118397

Hamraz, H., Contreras, M.A. & Zhang, J. (2017) A scalable approach for tree segmentation within small-footprint airborne LiDAR data. *Computers & Geosciences*, **102**, 139–147. https://doi.org/10.1016/j.cageo.2017.02.017

Hruska, R., Mitchell, J., Anderson, M. & Glenn, N.F. (2012) Radiometric and geometric analysis of Hyperspectral imagery acquired from an unmanned aerial vehicle. *Remote Sensing*, **4**, 2736–2752. https://doi.org/10.3390/rs4092736

JRC. (2011) *Riparian zones: where green and blue networks meet: pan-European zonation modelling based on remote sensing and GIS. European Commission*. LU: Joint Research Centre. Institute for Environment and Sustainability. Publications Office.

Ke, Y. & Quackenbush, L.J. (2011) A comparison of three methods for automatic tree crown detection and delineation from high spatial resolution imagery. *International Journal of*

Remote Sensing, **32**, 3625–3647. https://doi.org/10.1080/01431161003762355

Latella, M., Sola, F. & Camporeale, C. (2021) A density-based algorithm for the detection of individual trees from LiDAR data. *Remote Sensing*, **13**, 322. https://doi.org/10.3390/rs13020322

Li, W., Guo, Q., Jakubowski, M.K., Kelly, M. (2012). *A new method for segmenting individual trees from the Lidar point cloud*. https://doi.org/10.14358/PERS.78.1.75.

Lindberg, E. & Holmgren, J. (2017) Individual tree crown methods for 3D data from remote sensing. *Current Forestry Reports*, **3**, 19–31. https://doi.org/10.1007/s40725-017-0051-6

Lingua, A., Marenchino, D. & Nex, F. (2009) Performance analysis of the SIFT operator for automatic feature extraction and matching in photogrammetric applications. *Sensors*, **9**, 3745–3766. https://doi.org/10.3390/s90503745

Lowe, D.G. (1999) Object recognition from local scale-invariant features. In: *Proceedings of the seventh IEEE international conference on computer vision. Presented at the proceedings of the seventh IEEE international conference on computer vision*, Vol. **2**, pp. 1150–1157. https://doi.org/10.1109/ICCV.1999.790410

Malanson, G.P. (1993) *Riparian landscapes*. Cambridge: Cambridge University Press.

Michez, A., Piégay, H., Lisein, J., Claessens, H. & Lejeune, P. (2016) Classification of riparian forest species and health condition using multi-temporal and hyperspatial imagery from unmanned aerial system. *Environmental Monitoring and Assessment*, **188**, 146. https://doi.org/10.1007/s10661-015-4996-2

Moe, K.T., Owari, T., Furuya, N. & Hiroshima, T. (2020) Comparing individual tree height information derived from field surveys, LiDAR and UAV-DAP for high-value timber species in northern Japan. *Forests*, **11**, 223. https://doi.org/10.3390/f11020223

Mohan, M., Silva, C.A., Klauberg, C., Jat, P., Catts, G., Cardil, A. et al. (2017) Individual tree detection from unmanned aerial vehicle (UAV) derived canopy height model in an open canopy mixed conifer Forest. *Forests*, **8**, 340. https://doi.org/10.3390/f8090340

Naiman, R.J., McClain, M.E. & Décamps, H. (2005) *Riparia: ecology, conservation, and management of streamside communities, Aquatic ecology series*. Amsterdam: Elsevier, Academic Press.

Nyimbili, P., Demirel, H., Seker, D., Erden, T. (2016) Structure from motion (SfM) - approaches and applications. In: *Proceedings of the international scientific conference on applied sciences, Antalya, Turkey*. pp. 27–30

Panagiotidis, D., Abdollahnejad, A., Surový, P. & Chiteculo, V. (2017) Determining tree height and crown diameter from high-resolution UAV imagery. *International Journal of Remote Sensing*, **38**, 2392–2410. https://doi.org/10.1080/01431161.2016.1264028

Pearse, G.D., Dash, J.P., Persson, H.J. & Watt, M.S. (2018) Comparison of high-density LiDAR and satellite photogrammetry for forest inventory. *ISPRS Journal of Photogrammetry and Remote Sensing*, **142**, 257–267. https://doi.org/10.1016/j.isprsjprs.2018.06.006

Pouliot, D.A., King, D.J., Bell, F.W. & Pitt, D.G. (2002) Automated tree crown detection and delineation in high-resolution digital camera imagery of coniferous forest regeneration. *Remote Sensing of Environment*, **82**, 322–334. https://doi.org/10.1016/S0034-4257(02)00050-0

Roussel, J.-R., Auty, D., Coops, N.C., Tompalski, P., Goodbody, T.R.H., Meador, A.S. et al. (2020) lidR: an R package for analysis of airborne laser scanning (ALS) data. *Remote Sensing of Environment*, **251**, 112061. https://doi.org/10.1016/j.rse.2020.112061

Sačkov, I., Bucha, T., Király, G., Brolly, G. & Raši, R. (2014) Individual tree and crown identification in the danube floodplain forests based on airborne laser scanning data. In: Zagajevski, B., Kycko, M. and Reuter, R. (Eds.) *Proceedings of the 34th EARSeL Symposium*. Warsaw, Poland: EARSeL and University of Warsaw, pp. 6.20–6.26.

Salerno, L., Bassani, F., Camporeale, C. (2020). *Carbon sequestration in tropical meandering rivers (no. EGU2020-13731)*. Presented at the EGU2020, Copernicus meetings. https://doi.org/10.5194/egusphere-egu2020-13731.

Seitz, S.M., Curless, B., Diebel, J., Scharstein, D. & Szeliski, R. (2006) A comparison and evaluation of multi-view stereo reconstruction algorithms. In: *2006 IEEE computer society conference on computer vision and pattern recognition - volume 1 (CVPR'06). Presented at the 2006 IEEE computer society conference on computer vision and pattern recognition - volume 1 (CVPR'06)*. New York, NY, USA: IEEE, pp. 519–528. https://doi.org/10.1109/CVPR.2006.19

Shi, Y., Wang, T., Skidmore, A.K. & Heurich, M. (2020) Improving LiDAR-based tree species mapping in central European mixed forests using multi-temporal digital aerial colour-infrared photographs. *International Journal of Applied Earth Observation and Geoinformation*, **84**, 101970. https://doi.org/10.1016/j.jag.2019.101970

Skoglar, P., Orguner, U., Törnqvist, D. & Gustafsson, F. (2012) Road target search and tracking with Gimballed vision sensor on an unmanned aerial vehicle. *Remote Sensing*, **4**, 2076–2111. https://doi.org/10.3390/rs4072076

Solari, L., Van Oorschot, M., Belletti, B., Hendriks, D., Rinaldi, M. & Vargas-Luna, A. (2016) Advances on Modelling riparian vegetation-hydromorphology interactions: modelling vegetation-hydromorphology. *River Research and Applications*, **32**, 164–178. https://doi.org/10.1002/rra.2910

Sothe, C., Dalponte, M., Almeida, C.M.d., Schimalski, M.B., Lima, C.L., Liesenberg, V. et al. (2019) Tree species classification in a highly diverse subtropical Forest integrating UAV-based photogrammetric point cloud and

Hyperspectral data. *Remote Sensing*, **11**, 1338. https://doi.org/10.3390/rs11111338

Souza, A.M.O. & Johansen, K. (2009) Remote sensing applications in riparian areas. In: Arizpe, D., Mendes, A. & Rabaça, J.E. (Eds.) *Sustainable Riparian Zones: A Management Guide*. Valencia: Generalitat Valenciana, pp. 148–156.

Takahashi Miyoshi, G., Imai, N.N., Garcia Tommaselli, A.M., Antunes de Moraes, M.V. & Honkavaara, E. (2020) Evaluation of Hyperspectral multitemporal information to improve tree species identification in the highly diverse Atlantic Forest. *Remote Sensing*, **12**, 244. https://doi.org/10.3390/rs12020244

Torres-Sánchez, J., López-Granados, F. & Peña, J.M. (2015) An automatic object-based method for optimal thresholding in UAV images: application for vegetation detection in herbaceous crops. *Computers and Electronics in Agriculture*, **114**, 43–52. https://doi.org/10.1016/j.compag.2015.03.019

Turner, D., Lucieer, A. & Watson, C. (2012) An automated technique for generating Georectified mosaics from ultra-high resolution unmanned aerial vehicle (UAV) imagery, based on structure from motion (SfM) point clouds. *Remote Sensing*, **4**, 1392–1410. https://doi.org/10.3390/rs4051392

Vastaranta, M., Kankare, V., Holopainen, M., Yu, X., Hyyppä, J. & Hyyppä, H. (2012) Combination of individual tree detection and area-based approach in imputation of forest variables using airborne laser data. *ISPRS Journal of Photogrammetry and Remote Sensing*, **67**, 73–79. https://doi.org/10.1016/j.isprsjprs.2011.10.006

Vega, C., Hamrouni, A., El Mokhtari, S., Morel, J., Bock, J., Renaud, J.-P. et al. (2014) PTrees: a point-based approach to forest tree extraction from lidar data. *International Journal of Applied Earth Observation and Geoinformation*, **33**, 98–108. https://doi.org/10.1016/j.jag.2014.05.001

Wang, X.-H., Zhang, Y.-Z. & Xu, M.-M. (2019) A multi-threshold segmentation for tree-level parameter extraction in a deciduous Forest using small-footprint airborne LiDAR data. *Remote Sensing*, **11**, 2109. https://doi.org/10.3390/rs11182109

Wolf, B.-M. & Heipke, C. (2007) Automatic extraction and delineation of single trees from remote sensing data. *Machine Vision and Applications*, **18**, 317–330. https://doi.org/10.1007/s00138-006-0064-9

Xu, Z., Shen, X., Cao, L., Coops, N.C., Goodbody, T.R.H., Zhong, T. et al. (2020) Tree species classification using UAS-based digital aerial photogrammetry point clouds and multispectral imageries in subtropical natural forests. *International Journal of Applied Earth Observation and Geoinformation*, **92**, 102173. https://doi.org/10.1016/j.jag.2020.102173

Zörner, J., Dymond, J.R., Shepherd, J.D., Wiser, S.K. & Jolly, B. (2018) LiDAR-based regional inventory of tall trees—Wellington, New Zealand. Forests, **9**, 702. https://doi.org/10.3390/f9110702

Supporting Information

Additional supporting information may be found online in the Supporting Information section at the end of the article.

Appendix S1 SfM parameters and results.

